# Transboundary Marine Protected Areas as Adaptation to Climate Change

William Cheung, Juliano Palacios-Abrantes and Renato Molina\*

October 25, 2025

[Preliminary Draft]

#### Abstract

Marine ecosystems often span political boundaries, posing challenges for effective conservation and fisheries governance. We develop a dynamic bioeconomic model of transboundary fisheries management and assess how strategically placed marine protected areas (TMPAs) can mitigate the inefficiencies of decentralized decision-making. We calibrate the model using projections from a Dynamic Bioclimatic Envelope Model (DBEM) covering 43 species in the Tropical Eastern Pacific region under two climate scenarios (SSP1-2.6, SSP5-8.5). Our results highlight the conditions under which TMPAs improve welfare and conservation outcomes even in the absence of formal cooperation. These insights are timely as climate-driven range shifts alter the spatial distribution of shared marine resources.

## 1 Introduction

The progressive degradation of marine ecosystems due to overfishing, pollution, and climate change has underscored the need for effective conservation strategies. Marine Protected Areas (MPAs) have emerged as a pivotal tool in preserving marine biodiversity and ensuring the sustainability of ocean resources. However, the transboundary nature of many marine ecosystems presents unique challenges that single-nation MPAs cannot adequately address. In this work, we explore the development and implementation of Transboundary Marine Protected Areas (TMPAs), protected areas that span the maritime boundaries of two or more nations, as a means to foster cooperation and improve the management of shared marine resources.

Transboundary conservation is not a novel concept. Terrestrial examples such as the Waterton-Glacier International Peace Park between the United States and Canada illustrate the benefits of cross-border environmental collaboration (Ali, 2007). In the marine context, TMPAs remain relatively uncommon, despite their potential to protect migratory species, maintain ecological connectivity, and manage shared resources more effectively than isolated national efforts. The establishment of TMPAs aligns with international commitments, such as the Convention on Biological Diversity's Aichi Target 11, which calls for the conservation of at least 10% of coastal and marine areas through effectively and equitably managed, ecologically representative, and well-connected systems of protected areas (Bacon et al., 2019; Buchanan et al., 2020).

<sup>\*</sup>Cheung: University of British Columbia (w.cheung@oceans.ubc.ca). Molina: University of Miami (renato.molina@miami.edu) Palacios-Abrantes: University of British Columbia (j.palacios@oceans.ubc.ca)

Several existing TMPAs highlight the promise of this approach. The Sulu-Sulawesi Seascape, jointly managed by Indonesia, Malaysia, and the Philippines, integrates biodiversity protection with sustainable development objectives across a biologically rich and ecologically connected region (Horigue et al., 2012). Likewise, the Benguela Current Commission—established by Angola, Namibia, and South Africa—offers a model for regional ecosystem-based governance, demonstrating how coordinated efforts can improve fisheries management in shared waters (Hamukuaya, 2020).

The appeal of TMPAs lies in their multifaceted benefits. Ecologically, they enable the protection of entire ecosystems and migratory routes. Economically, they can support sustainable fisheries and tourism-based livelihoods. Politically, TMPAs may act as diplomatic instruments, fostering cooperation and reducing resource-related conflicts (Guerreiro et al., 2010). Yet, their implementation remains difficult. Differing legal frameworks, enforcement capacities, and economic priorities across countries often hinder coordination. Effective governance of TMPAs requires robust institutional design, equitable benefit-sharing, and inclusive stakeholder engagement (Gjerde and Rulska-Domino, 2012).

Climate change exacerbates these coordination challenges. A growing body of work shows that the majority of the world's exploited marine species already straddle multiple Exclusive Economic Zones (EEZs), and that climate-driven shifts in species distributions are altering their national shares (Palacios-Abrantes et al., 2020). These shifts are expected to accelerate, raising the risk of resource conflicts and undermining existing bilateral or regional management regimes (Palacios-Abrantes et al., 2022). While this literature highlights the ecological and geopolitical consequences of transboundary change, it offers limited guidance on spatial policy tools that might realign incentives in a fragmented management landscape.

This paper seeks to fill that gap. We develop a dynamic model of a shared fishery distributed across multiple jurisdictions and explicitly incorporate spatial closures as a policy lever. This framework allows us to assess how the strategic allocation of protection, through TMPAs, can mitigate the inefficiencies of decentralized management, even in the absence of formal cooperation. We operationalize the model using projected species distributions from a Dynamic Bioclimatic Envelope Model (DBEM), focusing on the Tropical Eastern Pacific, a region of both ecological importance and institutional complexity.

Overall, this study makes three contributions. First, it introduces a tractable model of decentralized marine resource governance with spatial heterogeneity and actor asymmetry. Second, it embeds the model in a climate-sensitive ecological setting using spatial projections of species distributions. Third, it applies this framework to assess the scope and limitations of TMPAs in aligning incentives and improving conservation outcomes under climate change. The results inform the design of multilateral agreements and the role of spatial policy in managing shared and shifting marine resources.

#### 2 Economic Model

There are  $i = \{1...M\}$  jurisdictions exploiting a joint stock. Each jurisdiction may possess the institutions to regulate fishing within its own waters, but those necessary for joint management are not in place. A jurisdiction without institutions is thus assumed to be under open access.

Time is discrete. In time step t, there is a period of harvest and a period of reproduction. The stock reproduces and redistributes uniformly across the fishing grounds. There is no migration of the stock during the harvest season.

Let  $X_t$  and  $H_t$  denote the total fish stock and total harvest at time t. The stock's biology follows Levhari and Mirman (1980), in which growth is governed by the single parameter  $0 < \alpha < 1$ :

$$X_{t+1} = (X_t - H_t)^{\alpha}. \tag{1}$$

The dynamics ensure that growth is concave in the stock level, which is also standardized to be between 0 and 1. Overall, growth potential is then decreasing in  $\alpha$  (Breton and Keoula, 2014; Costello and Molina, 2021).

Following Costello and Molina (2021), we assume that protected area in jurisdiction i is given by  $\lambda_i$ , and that the fishing grounds available at each jurisdiction are given by  $\gamma_i(\lambda_i)$ . It follows that  $\gamma'_i < 0$ , and that  $\gamma_i(0)$  would be the total fishing grounds without any protection.  $\gamma_i(\gamma_i(0)) = 0$  would imply total closure of the jurisdiction. The schedule of protected areas is given by  $\lambda$ .

Under uniform distribution, it follows that the "fishable" stock in jurisdiction i at time t,  $x_{it}$ , would be given by:

$$x_{it} = X_t \gamma_i(\lambda_i). \tag{2}$$

Jurisdiction i thus chooses harvest  $h_{it}$  every period, and enjoys concave and increasing benefits given by:

$$u_{it} = \log\left[h_{it}\right]. \tag{3}$$

These benefits are then discounted by asymmetric discount factor  $\delta_i$ .

For our derivations, it will prove convenient to define total within-jurisdiction escapement as  $e_{it}$ . Note that  $h_{it} = x_{it} - e_{it}$ , so choosing escapement is a one-to-one equivalent to choosing harvest. Following Costello and Molina (2021), we also denote total stock protected as  $m_t$ , which is a function of a designated fraction of the entire spatial distribution of the stock. Uniform distribution then ensures:

$$m_t = X_t \sum_{i=1}^{M} \lambda_i \tag{4}$$

Using this simple framework, we will explore two benchmark cases: the non-cooperative Nash equilibrium, and the cooperative equilibrium. Both of which are provided below.

## 2.1 Non-Cooperative Solution

Let us consider the case in which all jurisdictions behave non-cooperatively. All jurisdictions extract the resource seeking to maximize the net present value of the stream of benefits, taking other jurisdictions' actions as given. Each jurisdiction then implements the best response to all other jurisdictions' best responses. This behavior results in the non-cooperative extraction in Proposition 1:

**Proposition 1.** Optimal asymmetric non-cooperative escapement in jurisdiction  $i \in 1 : M$ ,  $e_i^N$ , as a function of protection schedule  $\lambda$  is linear in the overall stock level,  $X_t$ , and it is given by:

$$e_i^N = X_t f^N(\lambda) \; ; \; f^N(\lambda) = \max \left\{ X \left( \gamma_i(\lambda_i) - \frac{\Gamma + \Lambda}{\beta_i(1+b)} \right), 0 \right\},$$

with:

$$\beta_i = \frac{\alpha \delta_i}{1 - \alpha \delta_i}, \quad b = \sum_{i=1}^M \frac{1}{\beta_i}, \quad \Gamma = \sum_{i=1}^M \gamma_i(\lambda_i), \quad \Lambda = \sum_{i=1}^M \lambda_i.$$

*Proof.* See proof in Appendix A.

#### 2.2 Cooperative Solution

Consider the case in which all jurisdictions behave cooperatively. In this scenario, all jurisdictions extract the resource seeking to maximize the sum of net present values of the stream of benefits following Costello and Molina (2021). Note that this cooperative criteria is robust to the time inconsistency problem behind heterogeneous discount rates (Jackson and Yariv, 2015). This is because of the isoelastic nature of the log utility De-Paz et al. (2013); Breton and Keoula (2014). Bearing this useful property in mind, the optimal cooperative escapement is given in Proposition 2 below:

**Proposition 2.** Optimal asymmetric cooperative escapement in jurisdiction  $i \in 1 : M$ ,  $e_i^C$ , as a function of protection schedule  $\lambda$  is linear in the overall stock level,  $X_t$ , and it is given by:

$$e_i^C = X_t f_i^C(\boldsymbol{\lambda}) \; ; \; f_i^C(\boldsymbol{\lambda}) = \max \left\{ X \left( \gamma_i(\lambda_i) - \frac{\Gamma + \Lambda}{M + c} \right), 0 \right\},$$

with:

$$\beta_i = \frac{\alpha \delta_i}{1 - \alpha \delta_i}, \quad c = \sum_{i=1}^M \beta_i, \quad \Gamma = \sum_{i=1}^M \gamma_i(\lambda_i), \quad \Lambda = \sum_{i=1}^M \lambda_i.$$

#### 2.3 Protection as Relative Sizes

In the numerical analysis, it will prove useful to streamline the analysis and work with protected areas as a relative share of fishing grounds available in each jurisdiction. That is,  $0 \le \lambda_i \le 1$ , and  $\gamma_i(\lambda_i) = \gamma_i(0)(1 - \lambda_i)$ , so  $\gamma_i(1) = 0$ . Note that when this is case, the overall protected stock over time is now given by:

$$m_t = X_t \sum_{i=1}^{M} \gamma_i(0) \lambda_i, \tag{5}$$

and optimal escapements simplify as shown in Lemma 1:

**Lemma 1.** When the protection schedule,  $\lambda$ , prescribes relative protection sizes, such that  $\gamma_i(\lambda_i) = \gamma_i(0)(1-\lambda_i)$ , optimal asymmetric non-cooperative and cooperative escapement in jurisdiction  $i \in 1: M$ ,  $e_i^N$ , are still linear in the overall stock level,  $X_t$ , and are given by:

$$e_i^N = X_t f^N(\boldsymbol{\lambda}) \; ; \; f^N(\boldsymbol{\lambda}) = \max \left\{ X \left( \gamma_i(\lambda_i) - \frac{\Gamma_0}{\beta_i(1+b)} \right), 0 \right\},$$

and

$$e_i^C = X_t f_i^C(\boldsymbol{\lambda}) \; ; \; f_i^C(\boldsymbol{\lambda}) = \max \left\{ X \left( \gamma_i(\lambda_i) - \frac{\Gamma_0}{M+c} \right), 0 \right\},$$

with:

$$\beta_i = \frac{\alpha \delta_i}{1 - \alpha \delta_i}, \quad b = \sum_{i=1}^M \frac{1}{\beta_i}, \quad c = \sum_{i=1}^M \beta_i, \quad \Gamma_0 = \sum_{i=1}^M \gamma_i(0).$$

*Proof.* When  $\lambda$  prescribes relative sizes,  $\Gamma = \sum_{i=1}^{M} \gamma_i(0)(1-\lambda_i)$  and  $\Lambda = \sum_{i=1}^{M} \gamma_i(0)\lambda_i$ . When this is the case, it follows that  $\Gamma + \Lambda = \sum_{i=1}^{M} \gamma_i(0)$ .

## 3 Ecological model

We use a Dynamic Bioclimatic Envelope Model (DBEM) to project the spatial distribution and relative biomass of marine species under different climate scenarios from 1951 to 2100. While the DBEM's detailed structure and implementation are documented elsewhere (Cheung et al., 2016, 2022), we summarize its core components here. The model integrates four principal factors shaping marine species distributions: physiological tolerances, habitat suitability, species-specific depth and latitudinal ranges, and population dynamics. Environmental drivers include sea surface temperature, salinity, dissolved oxygen, and pH. For pelagic species, surface-level conditions are used; for demersal species, bottom ocean conditions are emphasized. The model also accounts for bathymetry, vertical and horizontal advection, and habitat associations (e.g., coral reefs, continental shelves, slope areas, and seamounts).

DBEM simulations are conducted on a global  $0.5^{\circ}$  latitude  $\times~0.5^{\circ}$  longitude grid. Within each cell, relative abundance is modeled using a logistic population growth function, influenced by species-specific growth parameters and spatial dispersal. Biomass is derived by multiplying relative abundance by individual body mass, which is dynamically adjusted via a temperature- and oxygen-sensitive von Bertalanffy growth model. Dispersal of both adults and larvae is governed by advection-diffusion-reaction equations. Larval dispersal is shaped by ocean currents (simulated by Earth System Models) and pelagic larval duration, estimated empirically. Adult movement is driven by density gradients and local carrying capacity, which is determined by environmental suitability and species mobility. For instance, highly mobile pelagic species like tuna disperse widely, while sessile organisms such as clams exhibit minimal movement. Simulations include a 100-year spin-up period (using climatological averages from 1951–2000) to stabilize the initial conditions.

We analyze DBEM output for 43 species, aggregating grid-level projections to Exclusive Economic Zones (EEZs) and the high seas. For this study, we focus on five EEZs: Colombia (Pacific), Panama (Pacific), Costa Rica (Pacific), the Galápagos Islands (Ecuador), and mainland Ecuador. All remaining ocean areas were classified as high seas. To reduce natural variability, we averaged relative biomass over four 20-year periods (Frölicher et al., 2016): a historical baseline (1995–2014), and three future windows (2021–2040, 2041–2060, and 2081–2100), representing early, mid-, and late-century projections, respectively. For each species, time period, and EEZ, we calculate relative biomass as the proportion of biomass in a given EEZ over the total biomass in the study area.

#### 3.1 Climate change scenarios

The DBEM was driven by output from three Earth System Models (ESMs) that participated in Phase 6 of the Coupled Model Intercomparison Project (CMIP6). These included GFDL-ESM4 (Geophysical Fluid Dynamics Laboratory), IPSL-CM6A-LR (Institut Pierre-Simon Laplace), and MPI-ESM1.2 (Max Planck Institute Earth System Model)(Dunne et al., 2020; Boucher et al., 2020; Gutjahr et al., 2019). Each ESM provided environmental forcing under two Shared Socioeconomic Pathway (SSP)

and Representative Concentration Pathway (RCP) combinations. The SSP1-2.6 scenario represents a low-emissions, high-mitigation future, with radiative forcing stabilizing at  $2.6 \text{ W/m}^2$  by 2100. In contrast, SSP5-8.5 reflects a high-emissions, low-mitigation pathway, with radiative forcing reaching 8.5 W/m<sup>2</sup> by the end of the century. Using multiple ESMs and emissions scenarios to drive the DBEM enables us to capture uncertainty stemming from both climate model structure and future socioeconomic trajectories (Frölicher et al., 2016).

## 4 Matching Extraction Incentives with TMPAs

To evaluate the practical effectiveness of transboundary marine protected areas (TMPAs), we conduct a policy experiment that integrates ecological projections with our theoretical bioeconomic model. Our goal is to estimate the spatial extent of protection necessary to reconcile decentralized, non-cooperative extraction with the socially optimal cooperative benchmark. We summarize our three-step approach below.

## 4.1 Estimating Species Parameters from DBEM Projections

We begin by translating ecological outputs from the Dynamic Bioclimatic Envelope Model (DBEM) into species-specific parameters for a surplus production model. For each species s, we extract time series of relative biomass  $B_{st}$  across the Tropical Eastern Pacific EEZs and estimate the intrinsic growth rate  $r_s$  and carrying capacity  $K_s$  using the logistic growth equation:

$$B_{s,t+1} = B_{st} + r_s B_{st} \left( 1 - \frac{B_{st}}{K_s} \right). (6)$$

To link this to our theoretical model, we simulate population dynamics implied by the logistic process and recover the equivalent parameter  $\alpha_s$  in the Levhari-Mirman form used in Equation 1. We do so by minimizing the sum of squared deviations between the normalized logistic trajectory and the path implied by  $X_{t+1} = X_t^{\alpha_s}$ , thus matching species-level growth responses.

## 4.2 Calibrating TMPA Size to Match Cooperative Escapement

Using the estimated  $\alpha_s$ , we solve for optimal escapement levels under both cooperative and non-cooperative regimes. For each species s, scenario k, and time horizon h, we compute:

- $e_{skh}^{C}$ : the cooperative escapement fraction, and
- $e_{skh}^{N}(\lambda)$ : the non-cooperative escapement when a TMPA of size  $\lambda \in [0,1]$  is imposed.

We then solve for the size of TMPA  $\lambda_{skh}^*$  that equates aggregate escapement across jurisdictions to the cooperative benchmark:

$$\lambda_{skh}^* = \arg\min_{\lambda \in [0,1]} \left( e_{skh}^C - e_{skh}^N(\lambda) \right)^2. \tag{7}$$

This calibration interprets the TMPA as a uniform spatial constraint applied across all jurisdictions sharing species s under scenario k and horizon h. Rather than relying on coordination, the TMPA shifts local incentives by restricting harvestable area, indirectly steering jurisdictions toward higher aggregate conservation. While allocations may differ from the cooperative optimum, the goal is to replicate its aggregate escapement through spatial policy alone.

#### 4.3 Optimal TMPA Sizes and Welfare Gains under Strategic Behavior

We next identify the TMPA size,  $\lambda \in [0, 1]$ , that maximizes global net present value (NPV) for each species s, scenario k, and horizon h, under decentralized decision-making. This defines:

$$\lambda_{skh}^* = \arg\max_{\lambda \in [0,1]} \text{NPV}_{skh}^{N+\text{TMPA}}(\lambda), \tag{8}$$

where the objective accounts for strategic responses to the TMPA, including changes in escapement and dynamic biomass feedback.

We compute this value numerically using our simulation model and summarize the distribution of  $\lambda_{skh}^*$  across all species and scenarios. This framework quantifies the spatial conservation effort needed to realign incentives under non-cooperative behavior. It provides both a theoretical benchmark and an empirical target for designing area-based policies in settings where full cooperation is limited or infeasible.

#### 5 Results

This section presents three main findings. First, we quantify the gap in conservation outcomes between cooperative and non-cooperative management regimes. Second, we estimate the uniform size of a transboundary marine protected area (TMPA) that, when imposed under non-cooperative behavior, replicates the average aggregate conservation achieved under cooperation. Third, we identify the TMPA size that maximizes global welfare, taking into account strategic responses and dynamic ecological feedbacks.

#### 5.1 Relative Gap in Conservation

Figure 1 presents the average conservation gap between cooperative and non-cooperative escapement across Exclusive Economic Zones (EEZs), aggregated over species, climate scenarios, and time horizons. For each EEZ, we report the mean difference in escapement rate, along with standard deviation error bars capturing cross-species and cross-scenario variability.

The results reveal substantial heterogeneity in the conservation shortfall associated with decentralized management across jurisdictions. The Galápagos Islands (Ecuador) exhibit the largest gap, averaging 6.6 percentage points, followed by Costa Rica (Pacific) at 6.4, Colombia (Pacific) at 5.8, and Panama (Pacific) and mainland Ecuador at 4.8 and 4.8, respectively. Standard deviations reflect greater heterogeneity in species-specific conservation needs.

While these gaps provide a useful benchmark for understanding the scope of inefficiencies under non-cooperative extraction, they should not be interpreted as direct targets for protection. Attempting to close these gaps through spatial closures alone would overlook the fact that strategic behavior under non-cooperative regimes may adapt in response. In other words, simply imposing the protection levels implied by cooperative behavior is unlikely to reproduce cooperative outcomes unless strategic dynamics are also addressed. This underscores the importance of explicitly accounting for behavioral responses when designing TMPAs.

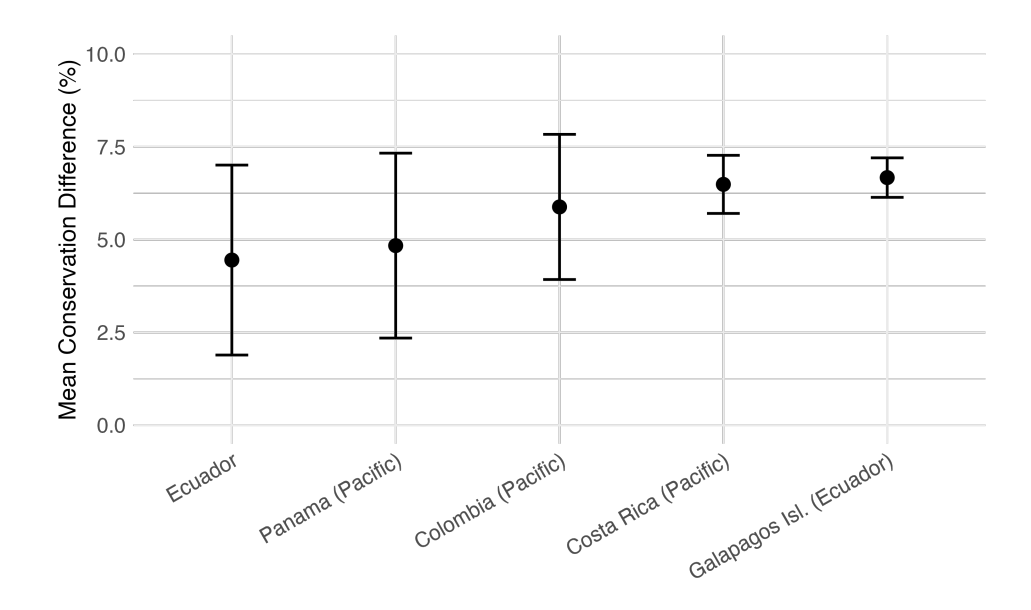


Figure 1: Average conservation gap across EEZs, measured as the difference in escapement rates between cooperative and non-cooperative outcomes. Error bars represent the standard deviation across species and scenarios.

#### 5.2 Distribution of Required TMPA Sizes for Escapement

We begin by analyzing the distribution of optimal transboundary marine protected area (TMPA) sizes, denoted  $\lambda_{sih}^*$ , that align non-cooperative escapement with the cooperative benchmark. These values are derived by solving for the uniform protection level that induces decentralized jurisdictions to voluntarily replicate the aggregate conservation achieved under coordination.

Figure 2 shows that optimal TMPA sizes vary substantially across species, scenarios, and jurisdictions. Note that a significant mass of the distribution lies above 70%, with the mean around 81%. This skewed pattern reflects structural asymmetries in jurisdictional biomass shares, species mobility, and biological growth captured through the estimated  $\alpha$  parameters.

These results reveal that even modest conservation gaps, such as an average escapement difference of five to ten percentage points as we demonstrated above, often require large uniform closures to be bridged. This is because a common protection level must overcome the weakest voluntary contributions, particularly from jurisdictions with low marginal incentives to conserve. In effect, uniform spatial rules must do more than equalize behavior; they must counteract strategic under-provision.

To provide further intuition: even when the aggregate gap between cooperative and non-cooperative escapement appears small, the underlying strategic behavior is highly asymmetric. Some jurisdictions contribute substantially to conservation even without coordination, while others contribute little or nothing, often because they hold a small share of biomass or face weak incentives due to limited ecological feedback. Moreover, under strategic behavior, jurisdictions adjust their actions in response to imposed TMPAs: as fishing grounds are protected, fishing intensity increases outside those areas.

A uniform TMPA must therefore compensate for both free-riding and strategic reallocation by imposing enough protection to discipline competition. The required protection level is not determined by the average shortfall but by the need to elevate the marginal contributions of the most under-conserving jurisdictions to meet the cooperative benchmark.

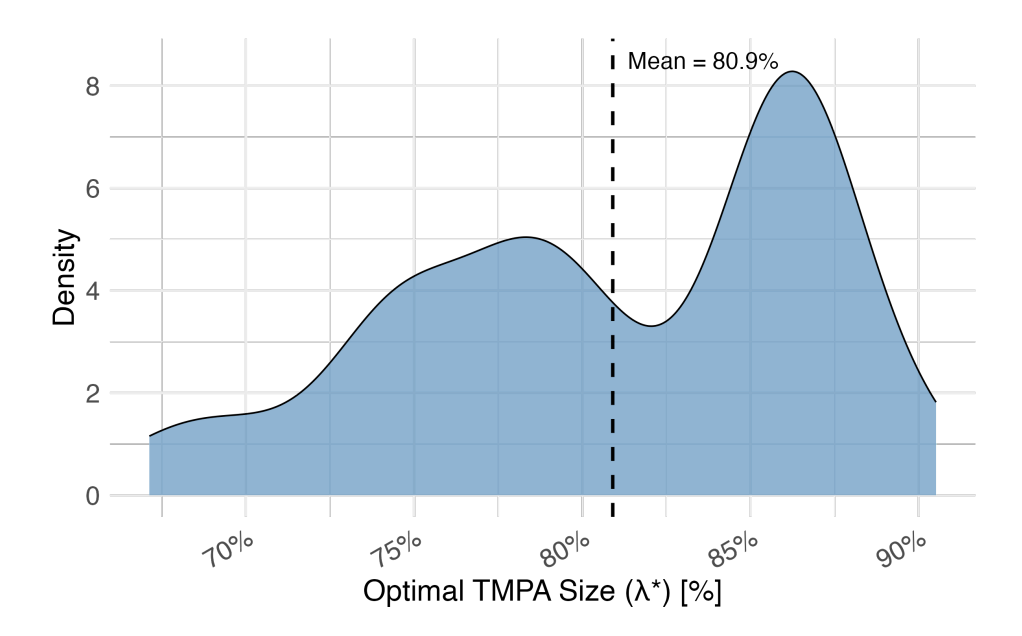


Figure 2: Distribution of optimal transboundary marine protected area (TMPA) sizes,  $\lambda^*$ , required to induce non-cooperative jurisdictions to match cooperative escapement levels. The dashed vertical line indicates the mean  $\lambda^*$  across all species, jurisdictions, scenarios, and horizons.

#### 5.3 Distribution of Required TMPA Sizes for Welfare

While conservation outcomes provide a static measure of ecological performance, they do not directly capture the economic incentives shaping jurisdictional behavior. To quantify the full value of cooperation, we simulate the net present value (NPV) of harvest benefits under each management regime using the dynamic bioeconomic model. For each species—scenario—horizon combination, we compare the welfare achieved under cooperative and non-cooperative extraction, initializing all simulations from a common biomass level derived from the early-century, low-emissions baseline. This approach isolates the effect of strategic behavior from initial ecological conditions.

Figure 3 presents the distribution of welfare gains from cooperation, expressed as the percentage improvement in discounted utility relative to the non-cooperative baseline. Specifically, we compute the percent gain as:

NPV Gain (%) = 
$$100 \times \frac{U^{\text{Coop}} - U^{\text{Non-Coop}}}{U^{\text{Non-Coop}}}$$
, (9)

where  $U^{\text{Coop}}$  and  $U^{\text{Non-Coop}}$  denote the present value of log harvest utility under cooperative and decentralized regimes, respectively.

The results demonstrate that cooperation delivers consistent welfare improvements, even when the absolute conservation gap is modest. On average, cooperative regimes reduce utility losses by 11% (mean value shown by the dashed line). However, the magnitude of gains varies across species and scenarios, reflecting heterogeneity in biological growth rates, discount factors, and strategic asymmetries.

These findings reinforce the case for institutional arrangements that promote joint management, not only to close ecological gaps but also to deliver substantial economic gains. They also underscore the limitations of spatial policy alone: while TMPAs can replicate aggregate conservation levels, they may not fully recover the dynamic welfare benefits of coordinated extraction paths.

Finally, we identify the transboundary marine protected area (TMPA) size that maximizes dynamic

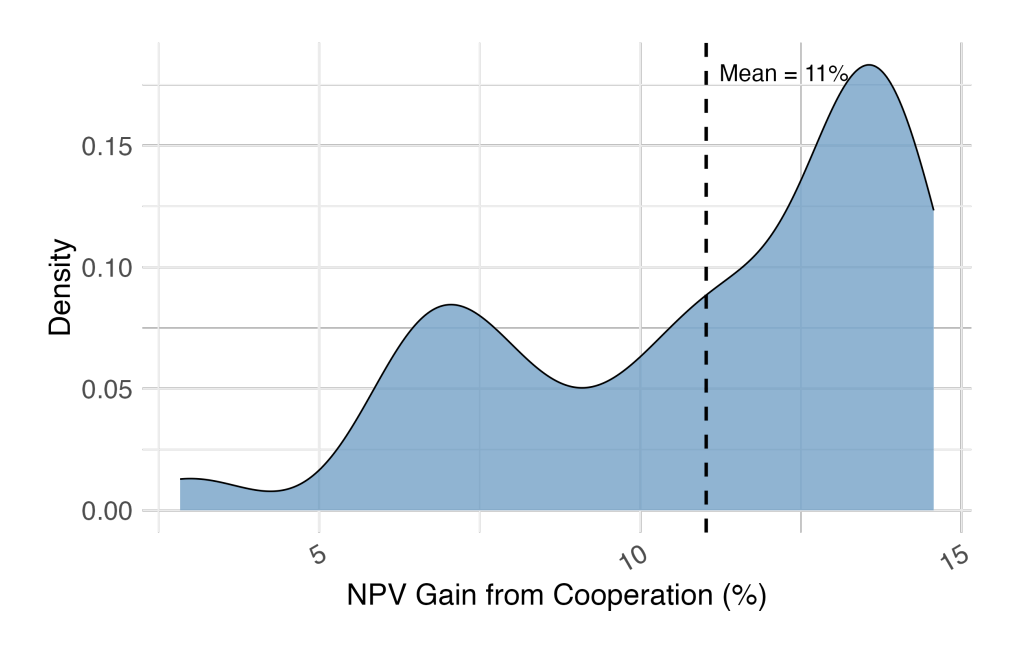


Figure 3: Distribution of welfare gains from cooperation, measured as the percentage improvement in net present value (NPV) of utility relative to the non-cooperative baseline. The dashed line indicates the mean gain across all simulations.

economic returns under strategic behavior. The results are shown in Figure 4, which summarizes the distribution of these welfare-maximizing TMPA sizes across species.

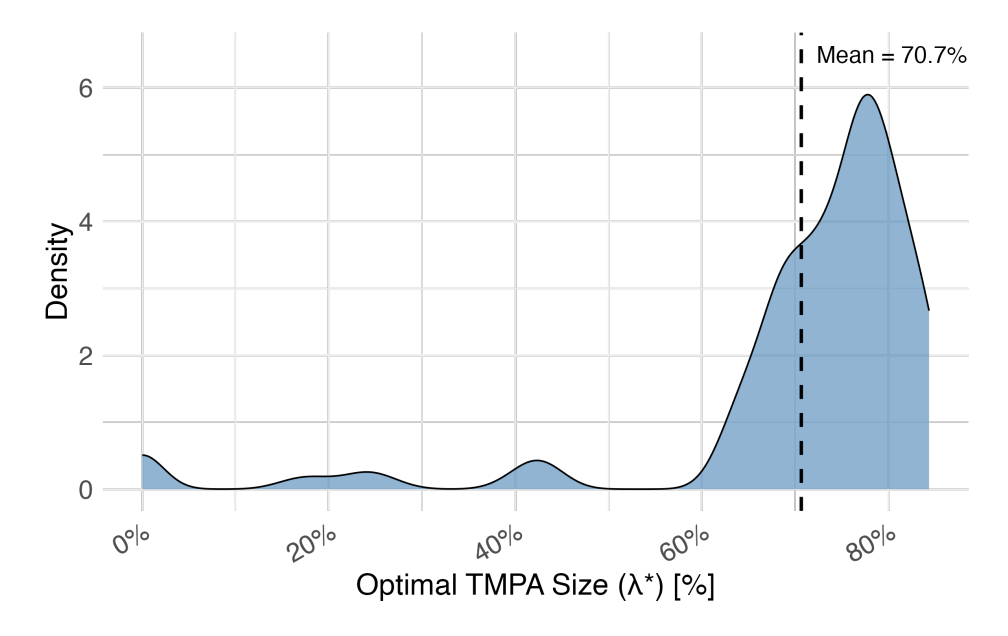


Figure 4: Distribution of welfare-maximizing TMPA sizes ( $\lambda^*$ ) across species, scenarios, and horizons. These values reflect the spatial protection levels that maximize dynamic utility under non-cooperative behavior. The dashed line indicates the mean value across all cases.

These results illustrate that While optimal sizes cluster around moderate-to-high protection levels (e.g., 60–80%), considerable variation emerges. In particular, some species, such as *Shortfin mako*, exhibit consistently low optimal TMPA sizes, reflecting limited benefits from spatial constraint due to high mobility and steep discounting.

These species-level optima provide a benchmark for tailoring spatial policy to ecological and economic conditions. WE note, however, that while uniform TMPAs may be easier to implement administratively, the heterogeneity observed here suggests that a species-specific approach could more efficiently recover welfare losses from uncoordinated extraction.

#### 6 Discussion and Conclusion

This study develops and applies a dynamic bioeconomic model to evaluate the performance of transboundary marine protected areas (TMPAs) under decentralized resource management. By linking ecological forecasts from the DBEM with a multi-agent game-theoretic framework, we quantify how uniform spatial closures interact with strategic behavior in shared fisheries. Our findings reveal several key insights for the design of spatial conservation policy under climate change.

First, cooperation delivers substantial improvements in both ecological and economic outcomes. These benefits arise not only from reduced harvest pressure but from aligning behavior across jurisdictions, thereby avoiding inefficient over-extraction and enabling more stable biomass trajectories. The welfare gains from cooperation are widespread, and in many cases large, even when the absolute differences in conservation metrics appear modest.

Second, our analysis of TMPAs as a spatial constraint reveals that inducing cooperative-like outcomes through uniform closures requires disproportionately large protected areas. This reflects the core strategic problem: non-cooperative agents respond to spatial policy by reallocating effort, not by passively absorbing conservation rules. As a result, the "gap-closing" TMPA sizes tend to be much larger than the escapement shortfall itself. This reinforces a central insight of our model; that the observed conservation deficit understates the size of the intervention required to offset strategic underprovision.

Third, when optimizing spatial protection to recover welfare rather than escapement alone, we find that a broad range of TMPA sizes are needed depending on species characteristics. While moderate-to-high protection levels often perform best, some species, particularly highly mobile or steeply discounted stocks, show limited welfare gains from spatial constraint. This heterogeneity highlights the potential inefficiency of blanket area-based targets, and suggests the value of tailoring TMPA design to ecological and economic context.

Taken together, these results underscore a broader policy lesson: maps do not manage people. Spatial protection that ignores strategic adaptation risks achieving far less than intended. Jurisdictions will respond to closures by intensifying effort elsewhere, shifting pressure rather than alleviating it. Effective TMPAs must not only protect space but also reshape incentives, either by coordinating behavior directly or by constraining it strongly enough to approximate cooperation.

In a world of shifting species and fragmented governance, TMPAs may serve as a second-best instrument for aligning incentives. But their design must be grounded in realistic models of behavior. The illusion of conservation through space alone can be dangerous if it obscures the need for deeper institutional coordination. Our framework offers a path to quantify and close that gap.

## References

- Ali, S. H. (2007). Peace parks: Conservation and conflict resolution. MIT press.
- Bacon, E., Gannon, P., Stephen, S., Seyoum-Edjigu, E., Schmidt, M., Lang, B., Sandwith, T., Xin, J., Arora, S., Adham, K. N., et al. (2019). Aichi biodiversity target 11 in the like-minded megadiverse countries. *Journal for Nature Conservation*, 51:125723.
- Boucher, O., Servonnat, J., Albright, A. L., Aumont, O., Balkanski, Y., Bastrikov, V., Bekki, S., Bonnet, R., Bony, S., Bopp, L., Braconnot, P., Brockmann, P., Cadule, P., Caubel, A., Cheruy, F., Codron, F., Cozic, A., Cugnet, D., D'Andrea, F., Davini, P., Lavergne, C., Denvil, S., Deshayes, J., Devilliers, M., Ducharne, A., Dufresne, J., Dupont, E., Éthé, C., Fairhead, L., Falletti, L., Flavoni, S., Foujols, M., Gardoll, S., Gastineau, G., Ghattas, J., Grandpeix, J., Guenet, B., Guez, Lionel, E., Guilyardi, E., Guimberteau, M., Hauglustaine, D., Hourdin, F., Idelkadi, A., Joussaume, S., Kageyama, M., Khodri, M., Krinner, G., Lebas, N., Levavasseur, G., Lévy, C., Li, L., Lott, F., Lurton, T., Luyssaert, S., Madec, G., Madeleine, J., Maignan, F., Marchand, M., Marti, O., Mellul, L., Meurdesoif, Y., Mignot, J., Musat, I., Ottlé, C., Peylin, P., Planton, Y., Polcher, J., Rio, C., Rochetin, N., Rousset, C., Sepulchre, P., Sima, A., Swingedouw, D., Thiéblemont, R., Traore, A. K., Vancoppenolle, M., Vial, J., Vialard, J., Viovy, N., and Vuichard, N. (2020). Presentation and Evaluation of the IPSL-CM6A-LR Climate Model. Journal of Advances in Modeling Earth Systems, 12(7).
- Breton, M. and Keoula, M. Y. (2014). A great fish war model with asymmetric players. *Ecological economics*, 97:209–223.
- Buchanan, G. M., Butchart, S. H., Chandler, G., and Gregory, R. D. (2020). Assessment of national-level progress towards elements of the aichi biodiversity targets. *Ecological Indicators*, 116:106497.
- Cheung, W. W., Jones, M. C., Reygondeau, G., Stock, C. A., Lam, V. W., and Frölicher, T. L. (2016). Structural uncertainty in projecting global fisheries catches under climate change. *Ecological Modelling*, 325:57–66.
- Cheung, W. W. L., Palacios-Abrantes, J., Frölicher, T. L., Palomares, M. L., Clarke, T., Lam, V. W. Y., Oyinlola, M. A., Pauly, D., Reygondeau, G., Sumaila, U. R., Teh, L. C. L., and Wabnitz, C. C. C. (2022). Rebuilding fish biomass for the world's marine ecoregions under climate change. Global Change Biology.
- Costello, C. and Molina, R. (2021). Transboundary marine protected areas. Resource and Energy Economics, 65:101239.
- De-Paz, A., Marín-Solano, J., and Navas, J. (2013). Time-consistent equilibria in common access resource games with asymmetric players under partial cooperation. *Environmental Modeling & Assessment*, 18:171–184.
- Dunne, J. P., Horowitz, L. W., Adcroft, A. J., Ginoux, P., Held, I. M., John, J. G., Krasting, J. P., Malyshev, S., Naik, V., Paulot, F., Shevliakova, E., Stock, C. A., Zadeh, N., Balaji, V., Blanton, C., Dunne, K. A., Dupuis, C., Durachta, J., Dussin, R., Gauthier, P. P. G., Griffies, S. M., Guo, H., Hallberg, R. W., Harrison, M., He, J., Hurlin, W., McHugh, C., Menzel, R., Milly, P. C. D., Nikonov, S., Paynter, D. J., Ploshay, J., Radhakrishnan, A., Rand, K., Reichl, B. G., Robinson, T., Schwarzkopf, D. M., Sentman, L. T., Underwood, S., Vahlenkamp, H., Winton, M., Wittenberg, A. T., Wyman, B., Zeng, Y., and Zhao, M. (2020). The GFDL Earth System Model Version 4.1

- (GFDL-ESM 4.1): Overall Coupled Model Description and Simulation Characteristics. *Journal of Advances in Modeling Earth Systems*, 12(11).
- Frölicher, T. L., Rodgers, K. B., Stock, C. A., and Cheung, W. W. L. (2016). Sources of uncertainties in 21st century projections of potential ocean ecosystem stressors. *Global Biogeochemical Cycles*, 30(8):1224 1243.
- Gjerde, K. M. and Rulska-Domino, A. (2012). Marine protected areas beyond national jurisdiction: some practical perspectives for moving ahead. *The International Journal of Marine and Coastal Law*, 27(2):351–373.
- Guerreiro, J., Chircop, A., Grilo, C., Viras, A., Ribeiro, R., and van der Elst, R. (2010). Establishing a transboundary network of marine protected areas: Diplomatic and management options for the east african context. *Marine Policy*, 34(5):896–910.
- Gutjahr, O., Putrasahan, D., Lohmann, K., Jungclaus, J. H., Storch, J.-S. v., Brüggemann, N., Haak, H., and Stössel, A. (2019). Max Planck Institute Earth System Model (MPI-ESM1.2) for the High-Resolution Model Intercomparison Project (HighResMIP). Geoscientific Model Development, 12(7):3241–3281.
- Hamukuaya, H. (2020). Benguela current convention supports ecosystem assessment and management practice. *Environmental Development*, 36:100574.
- Horigue, V., Aliño, P. M., White, A. T., and Pressey, R. L. (2012). Marine protected area networks in the philippines: Trends and challenges for establishment and governance. *Ocean & coastal management*, 64:15–26.
- Jackson, M. O. and Yariv, L. (2015). Collective dynamic choice: the necessity of time inconsistency. American Economic Journal: Microeconomics, 7(4):150–178.
- Levhari, D. and Mirman, L. J. (1980). The great fish war: an example using a dynamic cournot-nash solution. *The Bell Journal of Economics*, pages 322–334.
- Palacios-Abrantes, J., Frölicher, T. L., Reygondeau, G., Sumaila, U. R., Tagliabue, A., Wabnitz, C. C., and Cheung, W. W. (2022). Timing and magnitude of climate-driven range shifts in transboundary fish stocks challenge their management. *Global change biology*, 28(7):2312–2326.
- Palacios-Abrantes, J., Reygondeau, G., Wabnitz, C. C., and Cheung, W. W. (2020). The transboundary nature of the world's exploited marine species. *Scientific Reports*, 10(1):17668.

## Appendix

## A Proofs

## A.1 Non-Cooperative Escapement

*Proof.* Let  $V_{[e_i,e_{-i}]}(x_{it}): \mathbb{R}^+ \to \mathbb{R}$  be the total discounted benefits over an infinite time horizon as a function of the stock level available in each jurisdiction. Further, define the vector of parameters:

$$\beta_i \equiv \frac{\alpha \delta_i}{1 - \alpha \delta_i}.\tag{A.1}$$

Omitting time subscripts and adding a N superscript denoting "non-cooperative" for clarity, we will assume the value function takes the logarithmic form:

$$V_{[e_i,e_{-i}]}^N(x_i) = A_i^N + (1+\beta_i)\log[x_i], \ \forall \ i \in 1:M.$$
(A.2)

The maximization problem for each jurisdiction i, is to maximize the individual net present value of fishing benefits:

$$V_i^N(x_i) = \max_{e_i} \left\{ \log \left[ x_{it} - e_i \right] + \delta_i V_i^N(x_{i,t+1}) \right\}.$$
 (A.3)

Substitute equation (A.2) into (A.3):

$$V_i^N(x_i) = \max_{e_i} \Big\{ \log [X\gamma_i(\lambda_i) - e_i] + \delta_i \Big( A_i^N + (1 + \beta_i) \log[x_{i,t+1}] \Big) \Big\}, \tag{A.4}$$

and keep track that the stock dynamics are given by:

$$X_{t+1} = (e_1 + e_2 + \dots + e_M + m)^{\alpha}$$
, and  $m = X \sum_{i=1}^{M} \lambda_i$ .

Equation (A.4) can now be expressed as follows:

$$V_i^N(x_i) = \max_{e_i} \Big\{ \log \left[ X \gamma_i(\lambda_i) - e_i \right] + \delta_i A_i^N + \delta_i (1 + \beta_i) \gamma_i(\lambda_i) + \delta_i (1 + \beta_i) \alpha \log \left[ e_1 + e_2 + \dots + e_M + m \right] \Big\}. \tag{A.5}$$

Taking partials with respect to  $e_i$  and rearranging, gives the following first order condition for each jurisdiction i:

$$\frac{1}{X\gamma_i(\lambda_i) - e_i} = \frac{\delta_i(1 + \beta_i)\alpha}{e_1 + e_2 + \dots + e_M + m}.$$
(A.6)

Optimal escapement at jurisdiction i then satisfies:

$$e_i = X\gamma_i(\lambda_i) - \frac{e_1 + e_2 + \dots + e_M + m}{\delta_i(1 + \beta_i)\alpha}.$$
(A.7)

This is a system of M equations, which is straightforward to solve. First, let  $E = \sum_{i=1}^{M} e_i$  and note

that  $\delta_i(1+\beta_i)\alpha=\beta_i$ . Summing over all jurisdictions gives:

$$E = \sum_{i=1}^{M} X \gamma_i(\lambda_i) - \sum_{i=1}^{M} \frac{E+m}{\beta_i}.$$
 (A.8)

We can then group terms as follows:

$$E + \sum_{i=1}^{M} \frac{E}{\beta_i} = \sum_{i=1}^{M} X \gamma_i(\lambda_i) - m \sum_{i=1}^{M} \frac{1}{\beta_i}.$$
 (A.9)

Further, let  $b = \sum_{i=1}^{M} \frac{1}{\beta_i}$ ,  $\Gamma = \sum_{i=1}^{M} \gamma_i(\lambda_i)$ , and  $\Lambda = \sum_{i=1}^{M} \lambda_i$ . We can now substitute  $m = X\Lambda$ , and solve for total escapement:

$$E = X \frac{\Gamma - b\Lambda}{1 + b}. (A.10)$$

Substituting equation (A.10) into (A.7):

$$e_i = X\gamma_i(\lambda_i) - \frac{X\frac{\Gamma - b\Lambda}{1 + b} + X\Lambda}{\beta_i},$$
 (A.11)

which can then be simplified to:

$$e_i^N = X \left( \gamma_i(\lambda_i) - \frac{\Gamma + \Lambda}{\beta_i(1+b)} \right).$$
 (A.12)

This result implies that the equilibrium escapement is linear in the stock level, which verifies the guess in equation A.2. Recognizing that escapement cannot be negative, we can generalize the optimal escapement as function of the schedule of protected areas,  $\lambda$ , as follows:

$$e_i^N = X_t f^N(\lambda) \; ; \; f^N(\lambda) = \max \left\{ X \left( \gamma_i(\lambda_i) - \frac{\Gamma + \Lambda}{\beta_i(1+b)} \right), 0 \right\},$$
 (A.13)

with:

$$b = \sum_{i=1}^{M} \frac{1}{\beta_i}, \quad \Gamma = \sum_{i=1}^{M} \gamma_i(\lambda_i), \quad \Lambda = \sum_{i=1}^{M} \lambda_i.$$
 (A.14)

## A.2 Cooperative Escapement

*Proof.* Analog to the non-cooperative case, we will omit time subscripts and add a C superscript denoting "cooperative" for clarity. Assume the value cooperative function takes the logarithmic form:

$$V_{[e_i,e_{-i}]}^C(x_i) = A_i^C + (1+\beta_i)\log[x_i], \ \forall \ i \in 1:M.$$
(A.15)

Jurisdictions are altruistic, so the maximization problem for each jurisdiction i is to maximize the total

15

net present value of fishing benefits:

$$V_i^C(x_i) = \max_{e_i} \left\{ \sum_{i=1}^M \left( \log \left[ x_{it} - e_i \right] + \delta_i V_i^C(x_{i,t+1}) \right) \right\}.$$
 (A.16)

Substitute equation (A.15) into (A.16):

$$V_i^C(x_i) = \max_{e_i} \left\{ \sum_{i=1}^M \left( \log \left[ X \gamma_i(\lambda_i) - e_i \right] + \delta_i \left( A_i^C + (1 + \beta_i) \log[x_{i,t+1}] \right) \right) \right\}. \tag{A.17}$$

Recall that we can group total escapement as  $E = \sum_{i=1}^{M} e_i$ , and that  $\delta_i(1 + \beta_i)\alpha = \beta_i$ , so equation (A.17) can be written as:

$$V_i^C(x_i) = \max_{e_i} \left\{ \sum_{i=1}^M \left( \log \left[ X \gamma_i(\lambda_i) - e_i \right] + \delta_i A_i^N + \delta_i (1 + \beta_i) \gamma_i(\lambda_i) + \beta_i \log \left[ E + m \right] \right) \right\}.$$
 (A.18)

Let  $c = \sum_{i=1}^{M} \beta_i$ . Taking partials with respect to  $e_i$  and rearranging then gives:

$$\frac{1}{X\gamma_i(\lambda_i) - e_i} = \sum_{i=1}^M \left(\frac{\beta_i}{E+m}\right) = \frac{c}{E+m}.$$
(A.19)

Optimal cooperative escapement at jurisdiction i then satisfies:

$$e_i = X\gamma_i(\lambda_i) - \frac{E+m}{c}. (A.20)$$

Much like the non-cooperative case, this is a system of M equations. Let  $\Gamma = \sum_{i=1}^{M} \gamma_i(\lambda_i)$ , and  $\Lambda = \sum_{i=1}^{M} \lambda_i$ . Summing over all jurisdictions gives:

$$E = X\Gamma - \frac{M(E + X\Lambda)}{c} \tag{A.21}$$

Total escapement is then given by the following expression:

$$E = X \frac{\Gamma - M\Lambda/c}{1 + M/c}.$$
 (A.22)

Substituting equation (A.22) into (A.20):

$$e_i = X\gamma_i(\lambda_i) - \frac{X\frac{\Gamma - M\Lambda/c}{1 + M/c} + X\Lambda}{c}, \tag{A.23}$$

which can then be simplified to:

$$e_i^C = X \left( \gamma_i(\lambda_i) - \frac{\Gamma + \Lambda}{M + c} \right).$$
 (A.24)

This result implies that the equilibrium escapement is linear in the stock level, which verifies the guess in equation (A.2). Finally, we also need to note the possibility of corner solutions, so the cooperative

escapement for jurisdiction i is finally given by:

$$e_i^C = X_t f_i^C(\boldsymbol{\lambda}) \; ; \; f_i^C(\boldsymbol{\lambda}) = \max \left\{ X \left( \gamma_i(\lambda_i) - \frac{\Gamma + \Lambda}{M + c} \right), 0 \right\},$$
 (A.25)

with:

$$c = \sum_{i=1}^{M} \beta_i, \quad \Gamma = \sum_{i=1}^{M} \gamma_i(\lambda_i), \quad \Lambda = \sum_{i=1}^{M} \lambda_i.$$
 (A.26)